Polychromatic axial behavior of aberrated optical systems: Wigner distribution function approach

Walter D. Furlan, Genaro Saavedra, Enrique Silvestre, Pedro Andrés, and María J. Yzuel

We propose a new method for the computation of the tristimuli values that correspond to the impulse response along the optical axis provided by an imaging optical system working under polychromatic illumination. We show that all the monochromatic irradiance distributions needed for this calculation can be obtained from the Wigner distribution function associated with a certain version of the pupil function of the system. The use of this single phase-space representation allows us to obtain the above merit function for aberrated systems with longitudinal chromatic aberration and primary spherical aberration. Some numerical examples are given to verify the accuracy of our proposal. © 1997 Optical Society of America

1. Introduction

For assessing the performance of an optical imaging system working under broadband illumination, the classical monochromatic merit functions, such as the point-spread function (PSF) and the optical transfer function, should be extended to the polychromatic domain. This extension is usually carried out by the addition of a suitable number of monochromatic components weighted by the spectral distribution of the source and the color sensitivity of the receiver.

Often, the polychromatic axial response of the optical system is of major interest as a measure of the tolerance to aberrations. In particular, for visual optical systems—i.e., those in which the human eye is the final detector—the tristimuli values along the optical axis are used as a figure of merit.[1,2] These functions are derived from the axial values of the different monochromatic irradiance PSF's. Since analytical expressions for these PSF's are achievable for only a few simple pupil functions, several numerical methods to evaluate them have been developed.[3–5] However, the sequential calculation of the axial PSF's for every wavelength in the polychromatic case leads to a time-consuming procedure. On the other hand, some monochromatic merit functions have been expressed successfully in terms of different phase-space representations, such as the Wigner distribution function (WDF) or the ambiguity function.[6–9]

It is important to recognize that these approaches are especially useful when two circumstances take place together: First, a high number of monochromatic merit functions must be calculated for the same pupil function with different amounts of aberration, and second, all the above merit functions can be obtained from a single phase-space representation. In this way a technique for the calculation of the polychromatic optical transfer function of systems suffering from longitudinal chromatic aberration (LCA) has been proposed recently.[10]

Bearing in mind the above statements, in this study we propose a new method for the computation of the polychromatic axial response provided by an optical system with an arbitrary exit-pupil transmittance suffering from LCA and primary spherical aberration (SA). This approach needs only the WDF of the azimuthally averaged pupil function of the system to obtain all the values of the monochromatic axial irradiance PSF's we require to construct the polychromatic response along the optical axis. In Section 2 we give the theoretical basis of the method, and in Section 3 we present some numerical examples to illustrate its performance.

2. Basic Theory

The behavior of an optical imaging system under broadband illumination can be evaluated from the

W. D. Furlan, G. Saavedra, E. Silvestre, and P. Andrès are with the Departament d'Òptica, Universitat de València, E-46100 Burjassot, Spain. M. J. Yzuel is with the Departament de Física, Universitat Autònoma de Barcelona, E-08193 Bellaterra, Spain.

Received 14 February 1997; revised manuscript received 18 July 1997.

0003-6935/97/359146-06$10.00/0

polychromatic axial PSF, given the isoplanatism of the system. In particular, for visual systems the axial response can be assessed from the tristimuli values along the optical axis. These values are defined as a function of the defocus coefficient $\delta\omega_{20}$ by the weighted superpositions

$$X(\delta\omega_{20}) = \int_\lambda I(\delta\omega_{20};\lambda)\bar{x}_\lambda S(\lambda)\mathrm{d}\lambda, \tag{1a}$$

$$Y(\delta\omega_{20}) = \int_\lambda I(\delta\omega_{20};\lambda)\bar{y}_\lambda S(\lambda)\mathrm{d}\lambda, \tag{1b}$$

$$Z(\delta\omega_{20}) = \int_\lambda I(\delta\omega_{20};\lambda)\bar{z}_\lambda S(\lambda)\mathrm{d}\lambda, \tag{1c}$$

where $I(\delta\omega_{20};\lambda)$ is the axial monochromatic irradiance PSF, $S(\lambda)$ stands for the spectral distribution of the source, and $\bar{x}_\lambda$, $\bar{y}_\lambda$, and $\bar{z}_\lambda$ denote the spectral tristimuli values. These latter parameters can be considered as the chromatic-sensitivity functions of the human eye taken as a receiver for a given selection of the primary colors.

In general, we are involved in a two-step procedure for calculating numerically the polychromatic merit functions in Eqs. (1). The first step is to obtain, at discrete points along the axial interval of interest, the different monochromatic irradiance PSF's provided by the system for a suitably large number of wavelengths. The second step is the computation of the axial tristimuli values by means of the weighted superposition, evaluated in a discrete way, given by Eqs. (1). Usually, the first step is a time-consuming procedure, especially when a high accuracy is needed. Therefore an approach for reducing the computation time of the monochromatic irradiance PSF's is welcomed.

The amplitude monochromatic PSF along the optical axis for an imaging system is given for large Fresnel numbers by

$$\begin{aligned} p(\delta\omega_{20};\lambda) &= \frac{1}{\lambda}\int_0^{2\pi}\int_0^1 \mathbb{P}(r,\phi;\lambda)\exp\left(\frac{i2\pi}{\lambda}\delta\omega_{20}r^2\right)r\mathrm{d}r\mathrm{d}\phi \\ &= \frac{1}{\lambda}\int_0^{2\pi}\int_0^1 \tau(r,\phi)\exp\left\{\frac{i2\pi}{\lambda}\right. \\ &\quad \left.\times[\omega(r,\phi;\lambda)+\delta\omega_{20}r^2]\right\}r\mathrm{d}r\mathrm{d}\phi, \end{aligned} \tag{2}$$

where $\mathbb{P}(r,\phi;\lambda)$ is the generalized pupil function of the system, (r,ϕ) are the normalized polar coordinates at the exit-pupil plane, $\tau(r,\phi) = |\mathbb{P}(r,\phi;\lambda)|$, and $\omega(r,\phi;\lambda)$ is the wave-aberration function. We assume that the chromatic variations of the modulus of the generalized pupil function are negligible, i.e., the function $\tau(r,\phi)$ has no dependence on λ. If the system suffers from only SA and LCA, the aberration function is reduced to

$$\omega(r,\phi;\lambda) = \omega_{20}(\lambda)r^2 + \omega_{40}(\lambda)r^4, \tag{3}$$

where $\omega_{20}(\lambda)$ and $\omega_{40}(\lambda)$ are the LCA and SA coefficients, respectively. In this case, the axial monochromatic irradiance PSF can be expressed as a function of a single radial integral, as follows:

$$\begin{aligned} I(\delta\omega_{20};\lambda) &= |p(\delta\omega_{20};\lambda)|^2 \\ &= \frac{1}{\lambda^2}\left|\int_0^1 \tau_0(r)\exp\left(\frac{i2\pi}{\lambda}\{[\delta\omega_{20}+\omega_{20}(\lambda)]r^2\right.\right. \\ &\quad \left.\left.+\omega_{40}(\lambda)r^4\}\right)r\mathrm{d}r\right|^2, \end{aligned} \tag{4}$$

where $\tau_0(r)$ is the azimuthal average of $\tau(r,\phi)$.[11] By performing the change of variable $\mu = r^2$, we obtain

$$\begin{aligned} I(\delta\omega_{20};\lambda) &= \frac{1}{\lambda^2}\left|\int_0^1 q_0(\mu)\exp\left(\frac{i2\pi}{\lambda}\right.\right. \\ &\quad \left.\left.\times\{[\delta\omega_{20}+\omega_{20}(\lambda)]\mu+\omega_{40}(\lambda)\mu^2\}\right)\mathrm{d}\mu\right|^2 \\ &= \frac{1}{\lambda^2}\int_0^1\int_0^1 q_0(\mu)q_0^*(\mu')\exp\left(\frac{i2\pi}{\lambda}\right. \\ &\quad \times\{[\delta\omega_{20}+\omega_{20}(\lambda)](\mu-\mu')+\omega_{40}(\lambda) \\ &\quad \left.\times(\mu^2-\mu'^2)\}\right)\mathrm{d}\mu\mathrm{d}\mu', \end{aligned} \tag{5}$$

where $q_0(\mu) = \tau_0(r)$. Using the transformation $x = (\mu+\mu')/2$ and $x' = \mu-\mu'$ causes Eq. (5) to result, except for an irrelevant constant factor, in

$$\begin{aligned} I(\delta\omega_{20};\lambda) &= \frac{1}{\lambda^2}\int_{-\infty}^{+\infty}\left(\int_{-\infty}^{+\infty} q_0\left(x+\frac{x'}{2}\right)q_0^*\left(x-\frac{x'}{2}\right)\right. \\ &\quad \times\exp\left\{i2\pi\left[\frac{\delta\omega_{20}+\omega_{20}(\lambda)}{\lambda}\right.\right. \\ &\quad \left.\left.\left.+\frac{2\omega_{40}(\lambda)}{\lambda}x\right]x'\right\}\mathrm{d}x'\right)\mathrm{d}x, \end{aligned} \tag{6}$$

where the integration limits have been extended to infinity, given the finite extension of the function $q_0(x)$. The inner integral in Eq. (6) can be recognized as the WDF of the one-dimensional function q_0,[12] namely

$$\begin{aligned} W_{q_0}(x,\nu) &= \int_{-\infty}^{+\infty} q_0\left(x+\frac{x'}{2}\right)q_0^*\left(x-\frac{x'}{2}\right) \\ &\quad \times\exp(-i2\pi\nu x')\mathrm{d}x'. \end{aligned} \tag{7}$$

Thus the axial monochromatic irradiance PSF can be written as a line integral of the above WDF, where

the spatial-frequency variable ν is related by a linear transformation with the spatial variable x. Mathematically,

$$I(\delta\omega_{20};\lambda) = \frac{1}{\lambda^2}\int_{-\infty}^{+\infty} W_{q_0}[x, m(\lambda)x + n(\lambda)]\mathrm{d}x, \quad (8)$$

where

$$m(\lambda) = -\frac{2\omega_{40}(\lambda)}{\lambda}, \quad (9a)$$

$$n(\lambda) = -\frac{\delta\omega_{20} + \omega_{20}(\lambda)}{\lambda}. \quad (9b)$$

From Eqs. (8) and (9) we infer that all the values of the axial irradiance PSF for every wavelength and for any value of LCA and SA can be obtained from a single two-dimensional representation, namely the WDF of the mapped pupil $q_0(x)$. This result can be achieved by integration of the values of W_{q_0} along straight lines in the phase-space domain. The slope and the y intersect of these lines are fixed by the value of the aberration coefficients and by the wavelength of the light [see Eqs. (9)]. Moreover, the same WDF provides all the information needed to assess the axial behavior of the system for any scaled version of the pupil function, since they all lead to the same $q_0(x)$. If the pupil of the system presents no amplitude variations, the study of the system for different values of its numerical aperture can be carried out with the same phase-space function.

The present study can be extended in a straighforward manner to cases in which other aberrations—apart from the LCA and SA—with negligible wavelength dependence are present in the wave-aberration function. In this situation the additional phase variations of the generalized pupil $\mathbb{P}(r, \phi; \lambda)$ should be joined with the function $\tau(r, \phi)$ to obtain the function $q_0(x)$.

Note that, because of the change of variable $\mu = r^2$, the axial values of the polychromatic irradiance PSF are determined by the one-dimensional mapped function q_0. Hence a two-dimensional phase-space representation contains the whole of the information to solve our problem, despite the fact that our starting function is a two-dimensional pupil. This is a singular result since the WDF doubles the number of variables of the original function as any other phase-space representation. Several relevant properties of the WDF are presented in Refs. 12–14 and the references cited therein.

3. Numerical Examples

For testing the method and its performance we evaluate the polychromatic axial response produced by an optical system with a clear circular pupil that suffers from two different aberration functions. In the first case we consider that the system is affected by only LCA, whose $\omega_{20}(\lambda)$ coefficient is shown in Fig. 1 (case 1). In the second situation, in addition to the previous LCA the system also suffers from SA with a constant coefficient of $\omega_{40}(\lambda) = 360$ nm (case 2).

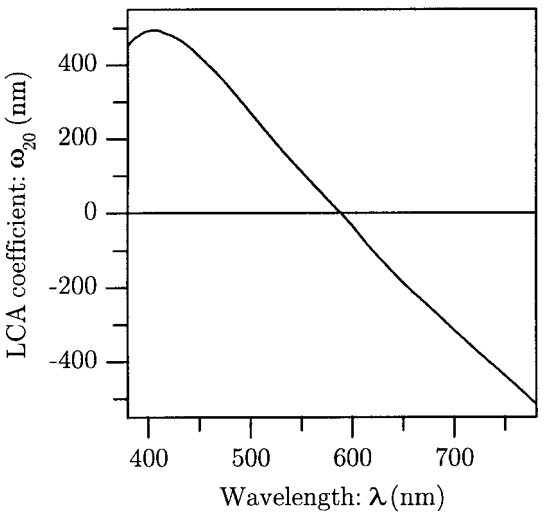

Fig. 1. Variation of the LCA coefficient that affects the system under study with λ.

As was pointed out in Section 2, we can discuss both situations starting from the same WDF associated with the function $q_0(x)$ of the system, which, in this case, is simply a rectangle function. The function $W_{q_0}(x, \nu)$ is digitally obtained by a sequence of fast Fourier transformations with a resolution of 4096×4096 points in the phase-space domain. A gray-scale picture of the modulus of this bidimensional function is shown in Fig. 2. From this result the axial values of the monochromatic PSF's are cal-

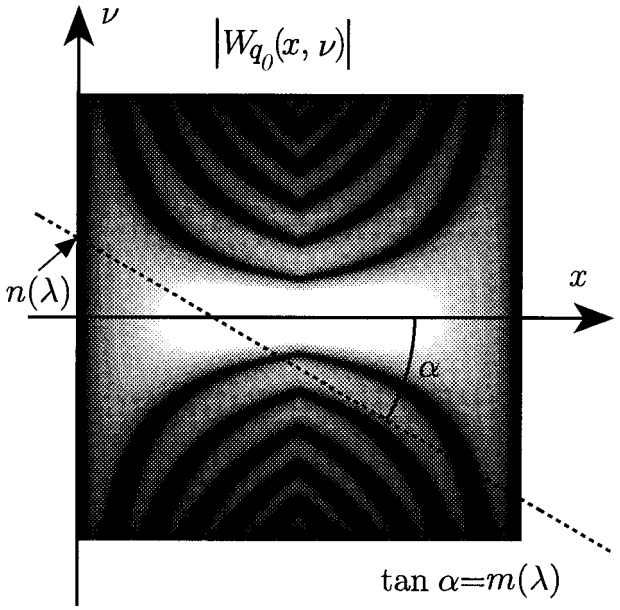

Fig. 2. Modulus of the WDF of the mapped pupil q_0 under consideration. A schematic representation of the integration lines cited in the main text is also shown, with $m(\lambda)$ and $n(\lambda)$ given by Eqs. (9).

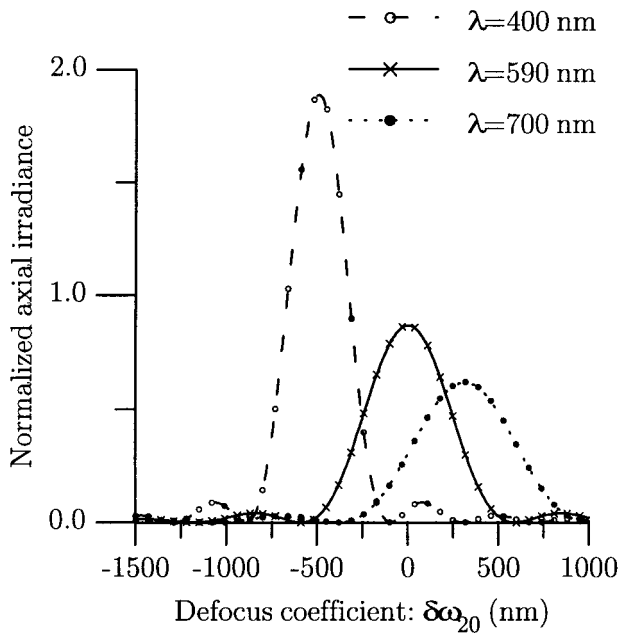

Fig. 3. Normalized monochromatic axial irradiance for three wavelengths of the optical system with a clear circular pupil and LCA shown in Fig. 1. The curves and symbols correspond to the theoretical and the computed results, respectively. The normalization is such that the maximum value of the irradiance for $\lambda = 550$ nm is unity.

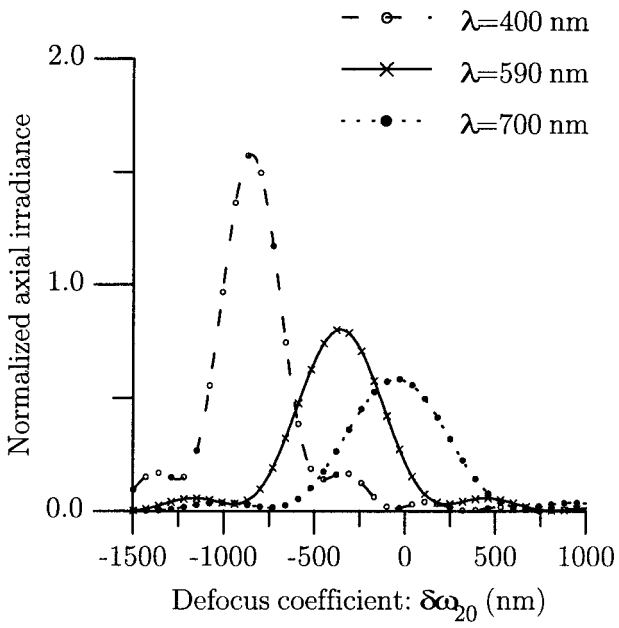

Fig. 4. Same as in Fig. 3, but here the system suffers from an additional SA with a constant coefficient of $\omega_{40}(\lambda) = 360$ nm.

culated by numerical integration along the straight lines fixed by the parameters given by Eqs. (9).

For the system at issue it is possible to obtain an analytical expression for the axial monochromatic irradiance PSF's for both aberration functions. This theoretical result is used to assess the accuracy of the proposed technique for the calculation of the monochromatic components. For case 1 [$\omega_{40}(\lambda) = 0$], the theoretical result is

$$I(\delta\omega_{20};\lambda) = \frac{1}{\lambda^2}\,\mathrm{sinc}^2\left[\frac{\delta\omega_{20} + \omega_{20}(\lambda)}{\lambda}\right],$$

where $\mathrm{sinc}(x) = \sin(\pi x)/(\pi x)$. To show the agreement between the theoretical prediction and the data obtained with the technique we propose, we selected three different wavelengths within the visible spectrum. Both results are compared in Fig. 3 and show perfect matching between them.

We also perform the calculation of axial monochromatic irradiance for case 2. Since the mapped pupil function $q_0(x)$ remains unchanged, no further calculation of the WDF is needed. The result is obtained by a simple change, according to Eqs. (9), of the straight lines along which the WDF should be integrated. Here, the monochromatic axial irradiance PSF's also have an analytical expression in terms of the Fresnel integrals.[3] The theoretical result predicts, for each wavelength, an intensity maximum located at $\delta\omega_{20} = -[\omega_{20}(\lambda) + \omega_{40}(\lambda)]$. Figure 4 shows the perfect correspondence between the analytical result and the data obtained with our method.

Finally, the polychromatic response of the system is also computed for both cases 1 and 2. The spectral-sensitivity functions used in the computation of the axial tristimuli values correspond to those associated with the CIE 1931 standard observer, and we identify the spectral distribution of the source with the standard illuminant C. The integrals in Eqs. (1) are numerically evaluated with a sampling of 400 equally spaced wavelengths in the range 400 nm $\le \lambda \le$ 750 nm.

For comparison purposes we use the results presented in Ref. 15 for the same systems. In that research the monochromatic irradiance PSF's were obtained by use of the classical method of Hopkins and Yzuel,[3] and Eqs. (1) were evaluated by direct numerical computation. For comparison with these results, an alternative description of the polychromatic axial behavior is used. In fact, instead of the tristimuli values we employ a conventional set of parameters derived from them, namely the normalized axial illuminance Y_N and the axial chromaticity coordinates x, y. These magnitudes are defined as a function of the defocus coefficient by

$$Y_N(\delta\omega_{20}) = \frac{Y(\delta\omega_{20})}{\displaystyle\int_\lambda (1/\lambda^2)\bar{y}_\lambda S_\lambda \mathrm{d}\lambda}, \tag{10}$$

$$x(\delta\omega_{20}) = \frac{X(\delta\omega_{20})}{X(\delta\omega_{20}) + Y(\delta\omega_{20}) + Z(\delta\omega_{20})}, \tag{11}$$

$$y(\delta\omega_{20}) = \frac{Y(\delta\omega_{20})}{X(\delta\omega_{20}) + Y(\delta\omega_{20}) + Z(\delta\omega_{20})}. \tag{12}$$

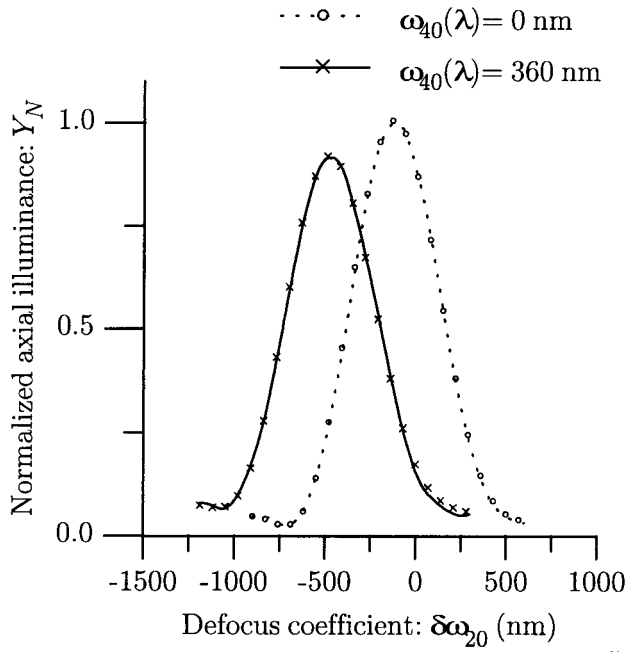

Fig. 5. Normalized axial illuminance as a function of $\delta\omega_{20}$ for the two systems under study. The solid and dotted curves represent the results shown in Ref. 15 obtained by use of the Hopkins and Yzuel method,[3] whereas the symbols correspond to the values obtained with the method we propose.

The results reported in Ref. 15 concerning the axial illuminance Y_N for cases 1 and 2 are plotted together with our numerical data in Fig. 5. A quantitative comparison shows that the relative difference, on average, for the computed axial positions in the central lobe is less than 2.5% for each curve. The axial chromaticity coordinates are shown graphically in a similar way in Fig. 6. As one can see from Fig. 6, the agreement between both results is again evident.

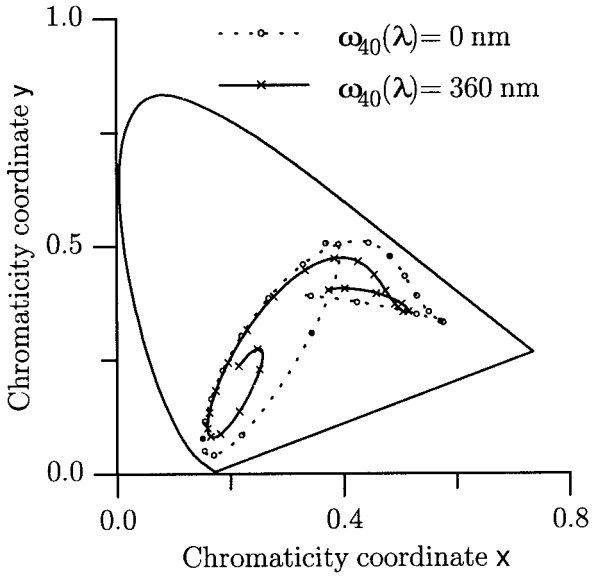

Fig. 6. Axial chromaticity diagram for the two systems under study. The notation used is the same as that for Fig. 5.

As was expected a considerable reduction in the computation time of the tristimuli values is achieved with the technique we propose. This is because all the monochromatic components needed for the calculation of the above parameters for both aberration types are obtained from a single representation of the pupil, whereas in the classical methods the entire calculation must be repeated for each axial position, wavelength, and aberration function. Although the calculation of $W_{q_0}(x, \nu)$ must be taken into account in the computation time, the ratio of this contribution to the total time is less and less important when a high number of axial positions, wavelengths, or both are involved.

4. Conclusions

An efficient method for the computation of the axial polychromatic impulse response provided by imaging systems suffering from LCA and SA has been proposed. The large amount of calculation time needed with the classical methods is reduced substantially by our approach because of the use of a single phase-space representation for obtaining all the data for the computation. This representation is the WDF of a certain mapped version of the azimuthally averaged pupil function of the system.

Numerical examples show that the accuracy of the method is high when compared with both analytical and numerical results obtained by other approaches. A detailed comparative analysis between the present method and others already reported requires the optimization of the corresponding algorithms, and therefore additional research is being carried out to quantify the savings in computation time yielded by our proposed technique for the same degree of accuracy.

Another outstanding feature of our approach is that two of the most common aberrations affecting optical systems, the LCA and the SA, become parameters, and consequently our formulation can be applied successfully for designing optical systems with low sensitivity to defocus, LCA, and SA.

This research has been supported by the Universitat de València (Projectes Precompetitius d'Investigació 1994). G. Saavedra was supported during this research by the Conselleria d'Educació i Ciència de la Generalitat Valenciana, Spain. E. Silvestre gratefully acknowledges the financial support of the Dirección General de Investigación Científica y Técnica (grant PB93-0354-C02-01), Ministerio de Educación y Ciencia, Spain.

References

1. M. J. Yzuel and J. Santamaría, "Polychromatic optical image. Diffraction limited system and influence of the longitudinal chromatic aberration," Opt. Acta **22,** 673–690 (1975).
2. M. J. Yzuel, J. C. Escalera, and J. Campos, "Polychromatic axial behavior of axial apodizing and hyperresolving filters," Appl. Opt. **29,** 1631–1641 (1990).
3. H. H. Hopkins and M. J. Yzuel, "The computation of diffraction patterns in the presence of aberrations," Opt. Acta **17,** 157–182 (1970).

4. J. J. Stamnes, B. Spjelkavik, and H. M. Pedersen, "Evaluation of diffraction integrals using local phase and amplitude approximations," Opt. Acta **30,** 207–222 (1983).
5. L. A. D'Arcio, J. J. M. Braat, and H. J. Frankena, "Numerical evaluation of diffraction integrals for apertures of complicated shape," J. Opt. Soc. Am. A **11,** 2664–2674 (1994).
6. K.-H. Brenner, A. W. Lohmann, and J. Ojeda-Castañeda, "The ambiguity function as a polar display of the OTF," Opt. Commun. **44,** 323–326 (1983).
7. J. Ojeda-Castañeda, P. Andrés, and E. Montes, "Phase-space representation of the Strehl ratio: ambiguity function," J. Opt. Soc. Am. A **4,** 313–317 (1987).
8. L. V. Bourimborde, W. D. Furlan, and E. E. Sicre, "Off-axis analysis of the Strehl ratio using the Wigner distribution function," J. Mod. Opt. **38,** 1685–1689 (1991).
9. D. Zalvidea, M. Lehman, S. Granieri, and E. E. Sicre, "Analysis of the Strehl ratio using the Wigner distribution function," Opt. Commun. **118,** 207–214 (1995).
10. W. D. Furlan, G. Saavedra, and J. Lancis, "Phase-space representations as a tool for the evaluation of the polychromatic OTF," Opt. Commun. **96,** 208–213 (1993).
11. M. Martínez-Corral, P. Andrés, and J. Ojeda-Castañeda, "On-axis diffractional behavior of two-dimensional pupils," Appl. Opt. **33,** 2223–2229 (1994).
12. M. J. Bastiaans, "The Wigner distribution function applied to optical signals and systems," Opt. Commun. **25,** 26–30 (1978).
13. M. J. Bastiaans, "Wigner distribution function and its application to first-order optics," J. Opt. Soc. Am. **69,** 1710–1716 (1979).
14. M. J. Bastiaans, "The Wigner distribution function and its application to optics," in *Optics in Four Dimensions–1980*, Vol. 65 of the AIP Conference Proceedings, M. A. Machado and L. M. Narducci, eds. (American Institute of Physics, New York, 1981), pp. 292–312.
15. J. Arlegui, "Estructura difraccional de la imagen policromática en sistemas ópticos: influencia de las aberraciones axiales," Ph.D. dissertation (Universidad de Zaragoza, Spain, 1973).